Biogeochemistry **27**: 129–152, 1994.

Sulfur and iron cycling in a coastal sediment: Radiotracer studies and seasonal dynamics

LARS MOESLUND[1], BO THAMDRUP[1] and
BO BARKER JØRGENSEN[2]*
[1] *Department of Microbial Ecology, Institute of Biological Sciences, Aarhus University, Ny Munkegade, DK-8000 Aarhus C, Denmark;* [2] *Max Planck Institute for Marine Microbiology Fahrenheitstr. 1, D-28359 Bremen, Germany; (* Author for correspondence)*

Received 10 January 1994; accepted 12 July 1994

Key words: iron reduction, marine sediment, radiotracer method, seasonal cycle, spring phytoplankton bloom, sulfate reduction

Abstract. The seasonal variation in sulfate reduction and the dynamics of sulfur and iron geochemistry were studied throughout a year in sediment of Aarhus Bay, Denmark. A radiotracer method for measuring sulfate reduction rates was applied with incubation times down to 15 min and a depth resolution down to 2 mm in the oxidized surface layer of the sediment. The radiotracer data were analyzed by a mathematical model which showed that, due to partial, rapid reoxidation of radioactive sulfide during incubation, the actual reduction rates in this layer were probably underestimated 5-fold. In the deeper, sulfidic zone, measured rates appeared to be correct. Sulfate reduction followed the seasonal variation in temperature with maximum activity at 1–2 cm depth in late summer. In spite of its rapid production, free H_2S was detectable in the porewater only below the depth of free Fe^{2+} at 6–7 cm throughout the year. Following the massive sedimentation from a spring phytoplankton bloom, anaerobic degradation of phytoplankton detritus was strongly stimulated over several weeks. A transient reversed redox zonation developed with a thin, black zone on top of the brown, oxidized sediment layer due to intensive sulfate and iron reduction. Mineralization through sulfate reduction was equivalent to two thirds of the annual net sedimentation of organic matter.

Introduction

Bacterial sulfate reduction is the predominant pathway of anaerobic mineralization of organic matter in coastal marine sediments. The sulfate reducing bacteria, however, compete with microorganisms using other electron acceptors in the upper sediment layers, and their activity is therefore regulated also by the availability of nitrate or of oxidized manganese and iron compounds (e.g. Aller & Rude 1988; Lovley 1991; Hines et al. 1991; Canfield et al. 1993a). In sediments containing large pools of manganese oxides or reactive iron oxides, these may become the main electron acceptors of the sediment (Aller et al. 1986; Canfield et al. 1993b).

The quantitative role of this competition between sulfate reduction and other respiratory processes in the oxidized surface layers is still poorly understood for organic-rich coastal sediments. The processes of manganese or iron reduction, of sulfate reduction, and of sulfide reoxidation by the metals may apparently occur in the same layers, and they are therefore difficult to dis-

criminate geochemically or to separate experimentally (e.g. Canfield et al. 1993a). Sulfate reducing bacteria have in recent years been found to occur in oxidized (i.e. having positive redox potential) and even oxic (i.e. containing O_2) sediment layers (Jørgensen & Bak 1991). By the use of particularly short incubation times in radiotracer experiments, or by trapping the produced radioactive sulfide, it has been possible in microbial mats to demonstrate sulfate reduction in the apparent presence of oxygen (Canfield & Des Marais 1991; Fründ & Cohen 1992; Jørgensen 1994). The regulation and seasonal variation of sulfate reduction in relation to other electron acceptors is therefore particularly interesting in the surface layers of sediments, where also the seasonal phytoplankton sedimentation has its most dynamic influence (e.g. Graf et al. 1982).

It was the goal of the present study to test the radiotracer method for sulfate reduction measurement in the oxidized layer of sediments and to understand the seasonal regulation of sulfate reduction, particularly in this zone. The results demonstrated seasonal dynamics which required frequent sampling and a mm depth resolution.

Materials and methods

All sediment samples were collected from Station 16 at 15 m water depth in the central Aarhus Bay, Denmark. (Jensen et al. 1988). The bay is situated on the transition between the brackish Baltic Sea and the North Sea, and the salinity at the bottom of the stratified water column varied during the period between 23‰ and 33‰ (Rasmussen & Jørgensen 1992). The sediment consisted of silty mud with a mean content of organic matter of 7% dry weight. Sediment cores of 20 cm length were collected without visible disturbance of the surface using a Haps corer. Sampling was done at 2–4 week intervals over one year, April 1988 to May 1989. Sediment cores were kept in the dark at *in situ* temperature under water from the sampling locality for about six hours before radiotracer measurements of sulfate reduction.

Radiotracer methods. Sulfate reduction rates were measured after each sampling occasion in nine parallel cores of 26 mm i.d. using $^{35}SO_4^{2-}$ tracer methods (Jørgensen 1978; Howarth & Jørgensen 1984; Fossing & Jørgensen 1989). The tracer was injected vertically from the top in the upper 0–2 cm and horizontally through fine silicone-stoppered holes in the side of the coring tubes at 2–12 cm depth. Carrier-free $^{35}SO_4^{2-}$ (3×15 μl of 75 kBq μl^{-1} in 3% NaCl) was injected vertically at three positions from the top of each core using a micromanipulator to ensure a controlled and even distribution of the tracer. Ten μl of the same tracer solution were injected through the side of the cores at 1 cm intervals.

Radiolabeled sediment cores were incubated at *in situ* temperature for 15, 40 and 120 min, respectively. For each incubation period, three cores were sectioned at depth intervals which increased from 2 mm at the surface to 1 cm in deeper layers. Zero-time controls were made by chilling sediment cores to 0 °C, injecting radiotracer, and then immediately sectioning and fixing the sediment. All sediment sections were rapidly transferred to centrifuge tubes and vortex-mixed with an equal volume of ice-cold 20% Zn-acetate. The bacterial sulfate reduction was thereby rapidly stopped and radiolabeled sulfides were fixed as ZnS. The samples were immediately frozen until the following separation of ^{35}S-labeled pools: SO_4^{2-}, AVS (Acid Volatile Sulfide), FeS_2 (pyrite) and S° (elemental sulfur).

The radioactivity of $^{35}SO_4^{2-}$ was determined on a 200 μl subsample of the supernatant after centrifugation of the thawn samples. The sediment was then washed with seawater and centrifuged twice to remove most of the remaining $^{35}SO_4^{2-}$. A 1 g subsample was acidified with ca. 6 N HCl under a stream of N_2, and AVS was driven as H_2S into 5% Zn-acetate traps. Subsequently, CRS (Chromium Reducible Sulfur; mostly FeS_2 and S°) was released as H_2S by addition of 0.5 M $CrCl_2$ in 1 N HCl and boiling for 45 min (Zhabina & Volkov 1978; Westrich 1983; Howarth & Jørgensen 1984; Canfield et al. 1986). Subsamples of $Zn^{35}S$ were taken from the traps for determination of AVS and CRS radioactivities.

Another subsample of the washed and centrifuged sediment was taken for extraction of S° by CS_2 (Troelsen & Jørgensen 1982). A 1 g sample was thoroughly homogenized with 2 ml 20% Zn-acetate and 6 ml CS_2 in a glass-stoppered centrifuge tube. After 24 h extraction and repeated homogenization, the suspension was centrifuged and a 2 ml subsample of pure CS_2 was carefully taken. The CS_2 was evaporated to dryness in a scintillation vial, the S° was redissolved in scintillation liquid, and the radioactivity was counted.

Chemical analyses. The pools of AVS and CRS were determined from the remaining ZnS in the distillation traps by the methylene blue method (Cline 1969). The pool of S° was determined from the CS_2 extracts by cyanolysis and spectrophotometry upon complexation with iron (Bartlett & Skoog 1954; Troelsen & Jørgensen 1982).

HCl-extractable iron was determined by extracting ca. 100 mg fresh sediment in 5 ml 0.5 N HCl for 1 h at 22 °C. Upon centrifugation, dissolved Fe^{3+} in the acidic supernatant was reduced to Fe^{2+} by addition of 1.5 M hydroxylamine hydrochloride in 0.25 M HCl at a ratio of 1:5. A 50 μl subsample was added to 2 ml 0.02% Ferrozine and the Fe^{2+} was determined spectrophotometrically at 562 nm (Stookey 1970; Sørensen 1982). This brief

extraction is selective for the amorphous or poorly crystalline fraction of the free iron oxides (Chao & Zhou 1983; Canfield 1988), but will also dissolve Fe(II)-minerals such as FeS and $FeCO_3$ and may leach some iron from silicates.

We attempted to separately measure Fe^{2+} and total Fe in the HCl extract for a calculation of HCl-extractable Fe(III), as has been done in other sediment studies (Lovley & Phillips 1986, 1987; Kostka & Luther 1994). By use of internal standards of ferrihydrite (poorly crystalline FeOOH) we, however, observed a significant reduction of Fe(III) to Fe(II) during the extraction so that this separation of oxidation states was not reliable. The reductant could be sulfides or organic compounds, and the problem increased with depth in the sediment. The experimental addition to sediment from 3–4 cm depth of 33 μmol Fe(III) g^{-1} sediment followed by immediate extraction thus increased the Fe^{2+} concentration in the extract by 15 μmol g^{-1} or by 52%.

Dissolved H_2S ('H_2S' = $H_2S + HS^- + S^{2-}$), SO_4^{2-}, and Fe^{2+} were determined in samples of porewater squeezed by N_2 from freshly sectioned sediment samples through (0.45 μm membrane filters. The first 1 ml was always discarded. Samples for H_2S were collected directly into 0.5% Zn-acetate and the sulfide was measured spectrophotometrically (Cline 1969). Samples from duplicate cores for SO_4^{2-} were collected in 0.5% $ZnCl_2$ to fix H_2S, refiltered, and the sulfate was determined by non-suppressed anion chromatography (Waters). Samples for Fe^{2+} were squeezed directly into 0.1% Ferrozine dissolved in 50 mM HEPES buffer at pH 7.0 and the Fe^{2+} was determined spectrophotometrically at 562 nm.

Results

Short-term $^{35}SO_4^{2-}$ reduction experiments. Incubations of sediment cores for 0, 15, 40, and 120 min showed a non-linearity with time over the first 15 min, which is important for the general interpretation of $^{35}SO_4^{2-}$ reduction experiments. The general trend of the time course experiments was similar over the different sampling dates over the seasons and a summary is shown here, calculated as the average of 4 × 15 incubated cores collected over the summer of 1988 and incubated for the above mentioned four lengths of time (Fig. 1). The graph shows sulfate reduction rates averaged over depth from the brown, oxidized surface layer at 0–1.5 cm depth and the black, reduced and sulfidic layer at 6–11 cm depth. Radiotracer incubations were done at five depths within each of these intervals and data were summed for Fig. 1, in which a constant zero-time blank radioactivity has been subtracted.

Due to natural heterogeneity in sulfate reduction activity, there was a relatively large scatter between the parallel cores. Yet, it was clear that in the reduced sediment, $^{35}SO_4^{2-}$ reduction proceeded linearly with time, while in

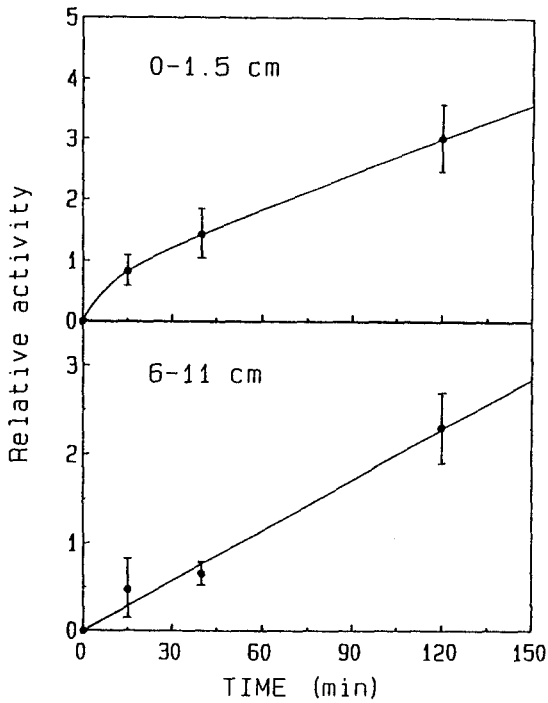

Fig. 1. Time course of $^{35}SO_4^{-2}$ reduction in the oxidized surface layer (upper frame) and the deeper reduced layer (lower frame) expressed in relative units of sulfate reduced. Sets of 3 parallel sediment cores for Aarhus Bay were incubated for different lengths of time at each of six sampling occasions during the period July–October 1988. Error bars show standard deviation of the mean for each incubation time.

the oxidized surface layer there was evidently a higher initial rate which then approached a lower, linear rate after about 15 min. A possible mechanism and explanation for these results is discussed in the Appendix based on a theoretical model.

Products of $^{35}SO_4^{2-}$ reduction. The reduced, ^{35}S-labeled products of sulfate reduction were analyzed in AVS, FeS_2, and S°. Figure 2 shows an example of the depth distribution of these labeled pools during spring 1988. Pyrite was the dominant radiolabeled product at the sediment-water interface where O_2 penetrated to 2 mm depth (Rasmussen & Jørgensen 1992). In the oxidized, suboxic zone at 0.2–2 cm depth, both FeS_2 and S° were important labeled products. In the deeper, reduced sediment, most of the reduced ^{35}S was recovered as AVS and the distribution of radiolabel in the three pools approached 70% in AVS, 20% in FeS_2, and 10% in S°.

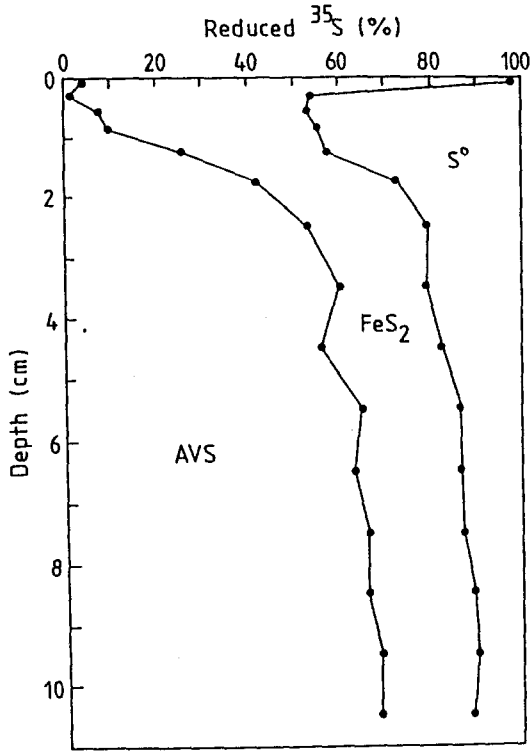

Fig. 2. Depth distribution of reduced, labeled products of $^{35}SO_4^{2-}$ reduction. The pools are shown as cumulative percent of ^{35}S in Acid Volatile Sulfide (AVS), pyrite (FeS_2), and elemental sulfur (S°) upon 40 min incubation of three parallel cores. May 9, 1988; 6 °.

Effects of a phytoplankton spring bloom. The sediment had a brown, oxidized surface layer which varied in thickness between 4 cm in winter and 2 cm in summer. Below this layer, the sediment was black due to a high iron sulfide content, but turned gray below 6–8 cm. Following a spring bloom of diatoms (mostly *Skeletonema costatum*) in the overlying water, there was a rapid phytoplankton sedimentation in April 1988, which was visible as a flocculent, brown film on the sediment surface. During the following weeks, a distinct, black band of a few mm thickness, visible in sediment cores taken in transparent Plexiglas tubes, appeared at the top of the brown, oxidized surface sediment. The black band was due to a highly stimulated sulfate reduction near the sediment surface and a resulting, transient accumulation of FeS near the top of the suboxic zone.

Oxygen now penetrated to only 1.5 mm depth (Rasmussen & Jørgensen 1992) while the brownish suboxic sediment layer reached 2 cm depth. There

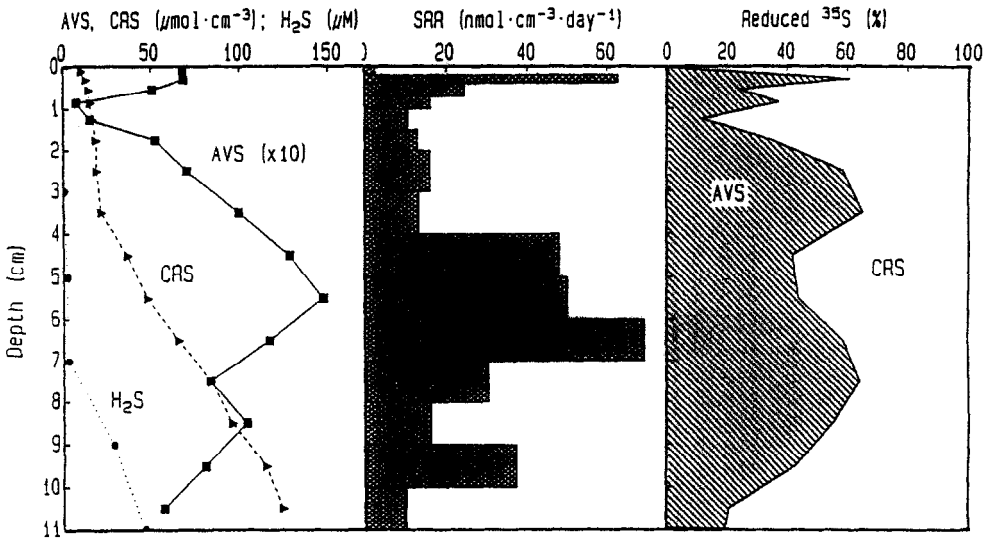

Fig. 3. Reduced sulfur pools and sulfate reduction following the sedimentation of a spring phytoplankton bloom. High FeS and sulfate reduction appeared in a narrow band just below the sediment-water interface overlying a more oxidized zone at 0.5–1.5 cm depth. *Left*: Pools of Acid Volatile Sulfide (concentrations exaggerated 10-fold), Chromium Reducible Sulfur, and free H_2S in the porewater. *Center*: Sulfate Reduction Rates, mean of 3 parallel cores. *Right*: Relative distribution of ^{35}S in reduced products of $^{35}SO_4^{2-}$ reduction. May 25, 1988; 7 °C.

was a local maximum of ca. 7 μmol FeS cm^{-3} in the uppermost 0–5 mm and a minimum at 1 cm below which FeS again accumulated (Fig. 3, left). There was no similar effect on the depth distribution of chromium reducible sulfur (mostly FeS_2) which occurred evenly in the upper 0–4 cm below which it accumulated with depth. Free H_2S near the detection limit was found at 5–7 cm, below which it accumulated in the porewater. Sulfate concentrations were 23–34 mM throughout the top 10 cm (data not shown).

Sulfate reduction also showed a sharp, local maximum of up to 64 nmol SO_4^{2-} cm^{-3} d^{-1} at 2–4 mm depth, which was of the same intensity as the maximal rates measured in the much broader sulfate reduction zone below 4 cm depth (Fig. 3, center). Thus, sulfate reduction in this surface maximum was obviously fed by organic matter from the rapidly degrading phytoplankton detritus, and it accounted for 8% of the overall reduction rate down to 11 cm depth. In accordance with the chemical pools, a high proportion of reduced ^{35}S was recovered as AVS just within the black surface band and also in the sulfidic sediment below 2 cm.

Seasonal dynamics of sulfur and iron. The large pools of inorganic sulfur and iron minerals showed general zonations that persisted throughout the

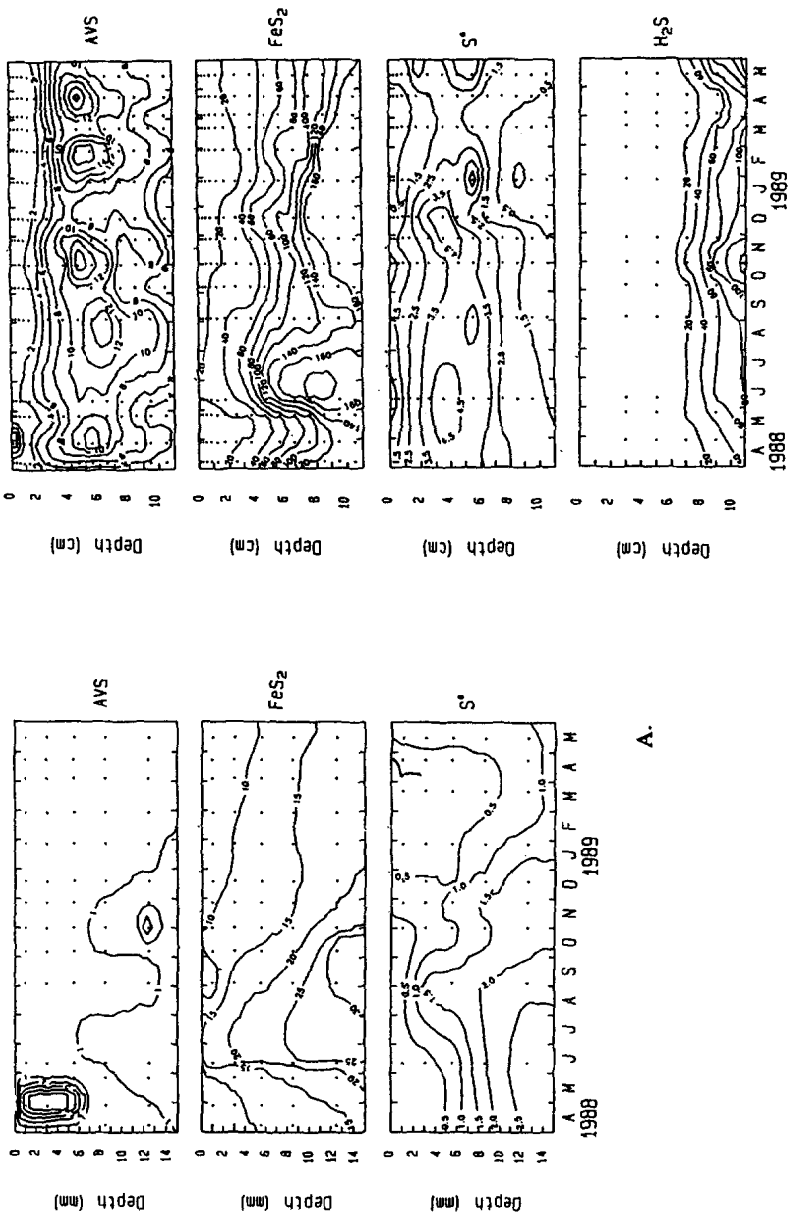

Fig. 4. Depth distribution of inorganic sulfur compounds in Aarhus Bay sediment over one year. Notice effects of sedimented phytoplankton bloom in spring 1988. A. Upper 0–15 mm. B. Upper 0–11 cm. Concentrations on isopleths are given in µmol S cm^{-3} sediment for solid phases and in µM for H_2S. Dots indicate depth and time of sampling.

year, overlain by perturbations due to seasonal variations in temperature and detritus sedimentation. The most distinct effect was the transient development of the thin reducing zone near the sediment-water interface in late April 1988 as the result of rapid sedimentation of the spring phytoplankton bloom (Fig. 4A). FeS accumulated up to 7 μmol S cm^{-3} in this black reducing band, which lasted for less than one month. In spring 1989, a similar rapid sedimentation of phytoplankton did not occur and no FeS band developed.

Within the uppermost 0–1.5 cm, the FeS built up during early summer and late fall where the oxidized zone was the thinnest, and it was oxidized again during winter (Fig. 4A). The main FeS zone at 4–7 cm depth showed a maximum of 10–15 μmol cm^{-3} at 5–6 cm with no clear seasonal variation (Fig. 4B). Pyrite accumulated during summer in the upper few cm and was gradually depleted again during winter, while elemental sulfur showed less clear seasonal variation. Throughout the year, free H_2S in the porewater only exceeded the detection limit of ca. 1 μM below 7 cm, probably due to bioturbation down to this depth which kept iron minerals partly in an oxidized, reactive state during all seasons.

The high spring sedimentation in 1988 also caused intensive iron reduction near the sediment-water interface. A local maximum of >200 μM Fe^{2+} was reached at that time just below the FeS band with a delay of a few weeks (Fig. 5). During the rest of the year, a Fe^{2+} maximum at 1–3 cm depth showed the continued iron reduction in this zone. The Fe^{2+} concentration decreased to <10 μM at 6–7 cm depth, coinciding with the upper boundary of detectable H_2S. The HCl-extractable iron was highest, 30–40 μmol cm^{-3}, in the oxidized zone at 1–2 cm depth throughout the year and showed only little seasonal variation. This maximum of extractable iron was about 3-fold higher than the FeS maximum a few cm below. It presumably represented the reactive iron pool, which occurred in oxidized form near the surface and in reduced form in the deeper layers. It reached a constant, low concentration in the H_2S zone below 6–7 cm depth, thus indicating the depletion of reactive iron.

Seasonal pattern of sulfate reduction. The spring bloom sedimentation in April 1988 resulted in intensive sulfate reduction in May within a thin sediment layer at 2–4 mm depth (Fig. 6A). Reduced ^{35}S was recovered in both the rapidly accumulating FeS and in FeS_2. The main sulfate reduction zone during spring 1988 occurred at 5–8 cm depth (Fig. 6B). During summer, it gradually moved upwards to 1–2 cm depth and increased in intensity to reach maximal activities of 190 nmol cm^{-3} d^{-1} in September. In accordance with the low AVS pool near the surface (Fig. 4), the maximal incorporation

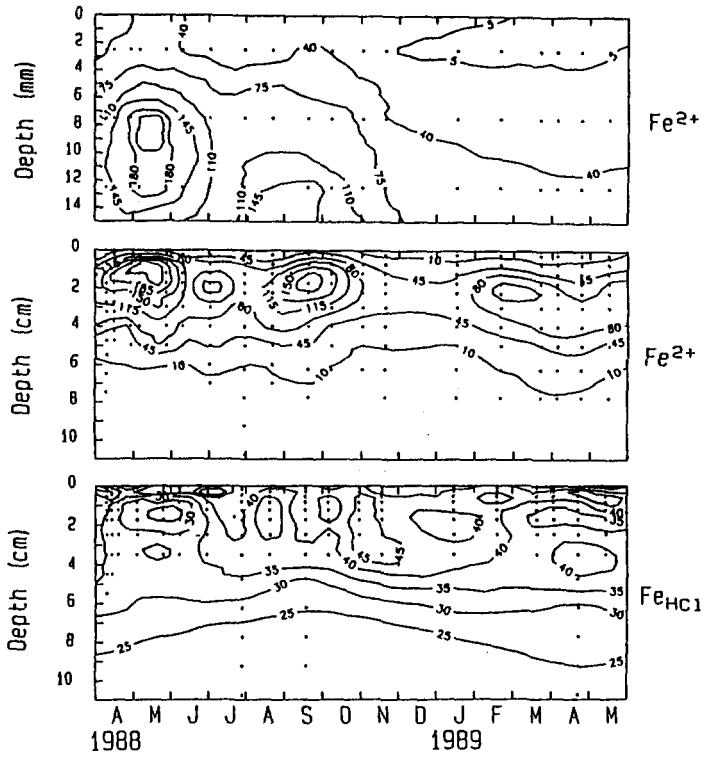

Fig. 5. Depth distribution of Fe^{2+} in the porewater and of HCl-extractable iron in Aarhus Bay sediment over one year. A near-surface Fe^{2+} maximum in May 1988 indicates intensive iron reduction as a result of a sedimented phytoplankton bloom. Concentrations on isopleths are given in μM for Fe^{2+} and in μmol cm^{-3} for Fe^{HCl}. Note different depth scales.

rate of reduced ^{35}S into FeS was found at 2–4 cm, deeper than the maximal incorporation into FeS_2 and S° which peaked at 1–2 cm.

From summer 1988 to spring 1989, the isopleth of 20 nmol cm^{-3} d^{-1} for total sulfate reduction in Fig. 6A coincided with the lower boundary of the O_2 zone which was 1.5 mm deep in summer and 5 mm deep in winter (Rasmussen & Jørgensen 1992). Thus, high sulfate reduction rates were measured within the brown, oxidized sediment just below the oxic zone, and sulfate reduction was also detectable within the oxic zone. Since FeS was not present in the most oxidized sediment, sulfate reduction was here detectable only from radioactivity accumulated in FeS_2 and S°.

Sulfate reduction rates were integrated over the top 0–1.5 cm and 0–11 cm in order to calculate the overall activity on an areal basis (Fig. 7). Integrated over the year, the sulfate reduction rate was 0.15 mol SO_4^{2-} m^{-2} y^{-1} from 0 to 1.5 cm depth and 1.75 mol SO_4^{2-} m^{-2} y^{-1} from 0 to 11 cm depth. Reduction

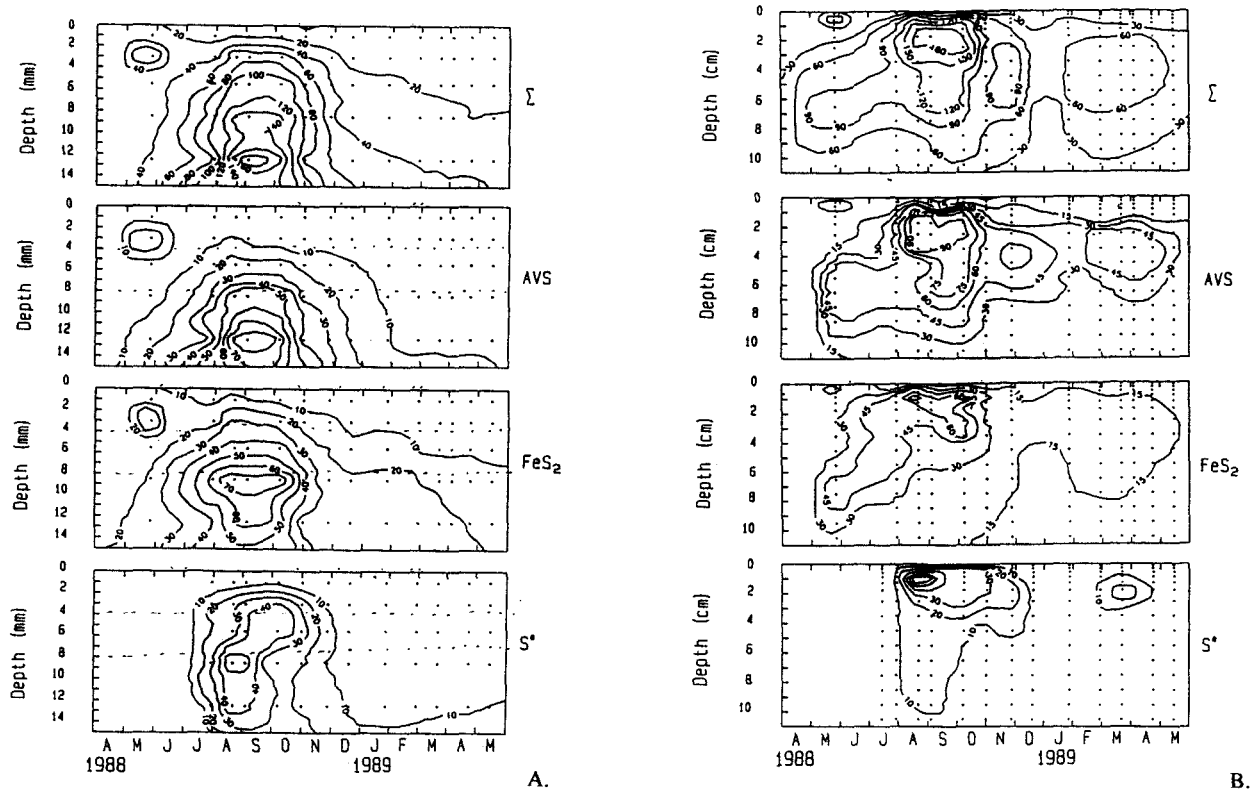

Fig. 6. Seasonal variations in bacterial sulfate reduction rates in Aarhus Bay sediment. The top frame shows the total reduction rates, based on the sum of radioactivities in the three pools, AVS, FeS_2, and S^0, while the three lower frames separately show the formation of ^{35}S-labeled AVS, FeS_2, and S^0, respectively, from $^{35}SO_4^{-4}$. Separate analysis of $^{35}S^0$ started only in July 1988. A. Upper 0–1.5 cm. B. Upper 0–11 cm. Reduction rates on isopleths are given in nmol SO_4^{2-} cm^{-3} d^{-1}. Incubation time was 40 min.

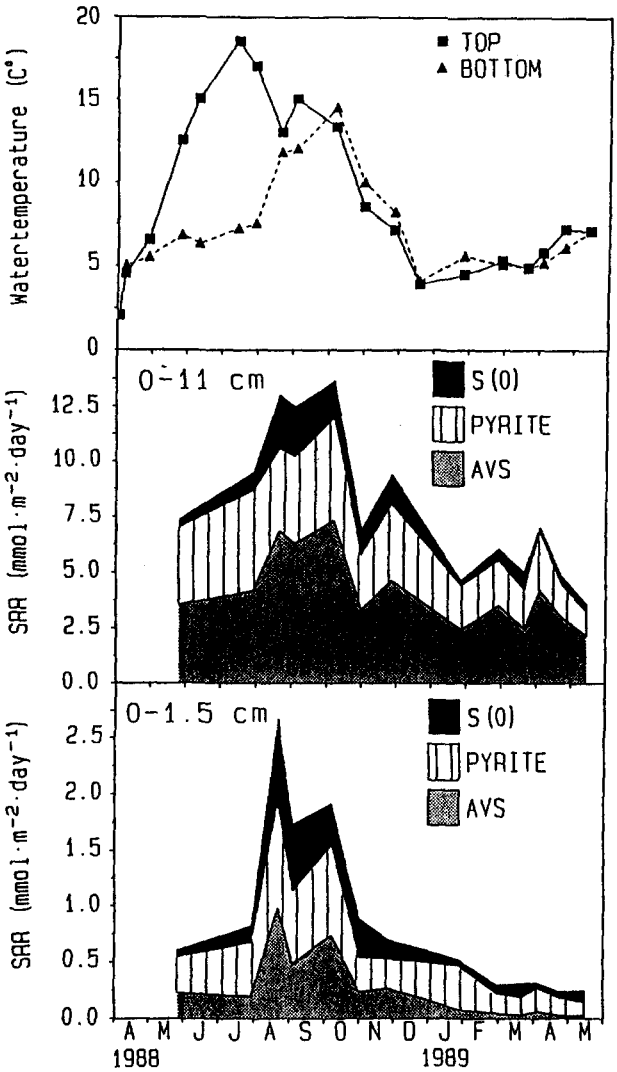

Fig. 7. Seasonal variations in water temperature and in sulfate reduction rates in Aarhus Bay. Top: Temperatures of surface water and of bottom water overlying the sediment. Center: depth integrated sulfate reduction rates in the upper 0–11 cm showing the allocation of reduced radiolabel in the AVS, pyrite, and S° pools. Bottom: the same for 0–1.5 cm depth.

rates varied in accordance with the *in situ* temperature. The bottom water, and thus the sediment, in Aarhus Bay was around 5 °C during winter and peaked at 14 °C during summer (Fig. 7). There was a 3-fold difference, 4–13 mmol m^{-2} d^{-1}, between summer and winter activity of sulfate reduction in the 11 cm thick sediment layer. Within the upper 1.5 cm, the seasonal variation

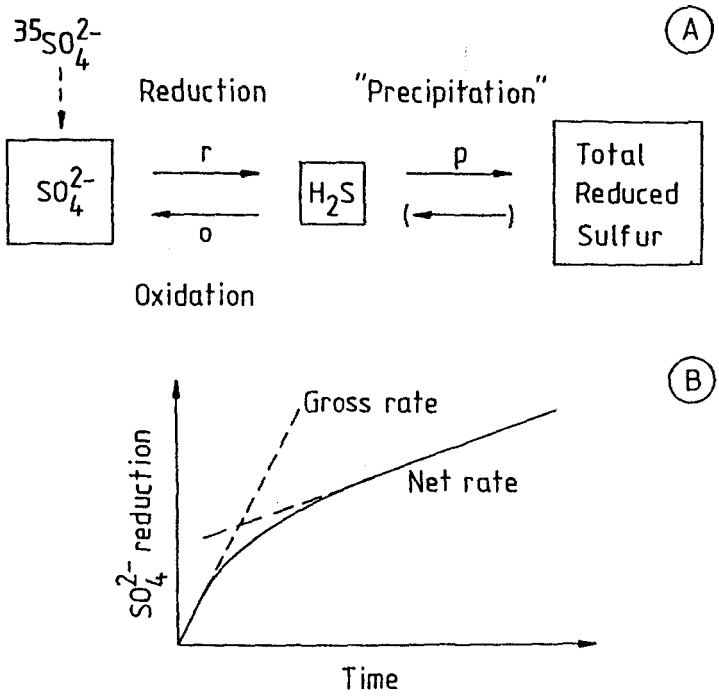

Fig. 8. A) Simplified model of those sulfur transformations, which affect the results of radiotracer determinations of sulfate reduction rates. B) Time course of gross and net sulfate reduction during a radiotracer experiment with partial reoxidation of sulfide.

with a high summer maximum was much more pronounced. Also the relative distributions of reduced ^{35}S varied significantly in the upper 0–1.5 cm where a large fraction of the radiolabel was recovered in the AVS pool only during late summer and fall. As a yearly average for the upper 1.5 cm, reduced ^{35}S was recovered with 25% in AVS, 46% in FeS_2, and 29% in S°. For the 0–11 cm layer, the numbers were 56% AVS, 32% FeS_2, and 12% S°. Of the overall sulfate reduction in the 0–11 cm layer, up to 20% occurred within the 0–1.5 cm surface layer during summer but only 7–8% during winter. Parallel data for these integrated values, obtained at the two incubation times, 40 min and 120 min, were similar within the standard error.

Discussion

Radiotracer method for sulfate reduction. Time-course experiments of $^{35}SO_4^{2-}$ reduction with short sediment incubations of 15–120 min showed linearity, i.e. constant reduction rate with time, in the black reducing zone at 6–11 cm depth (Fig. 1). In the oxidized surface layer at 0–1.5 cm, however, reduction

was apparently much faster at the beginning of incubation, and it then slowed down to reach a steady rate after about 15 min. To explain this reproducible non-linearity, we considered the possible radiotracer transformations during incubation and developed a simple model to describe these. The model is discussed in the Appendix and is shown graphically in Fig. 8. The model assumes steady-state of the non-radioactive pools and of process rates.

When a sulfate reduction experiment is carried out, $^{35}SO_4^{2-}$ is added in trace quantity to the large sulfate pool of the sediment (Fig. 8A). Labeled and non-labeled sulfate are reduced to H_2S, which has a very small pool size and a rapid turn-over. Some H_2S is reoxidized to sulfate and some is precipitated as Total Reduced Sulfur (TRS, excluding H_2S) in the form of FeS, FeS_2, or S°. Some of the radiolabel in H_2S is also transferred to the TRS pool by rapid isotopic exchange (Fossing et al. 1992). When the total amount of accumulated, reduced ^{35}S is analyzed after an incubation, the actual sulfate reduction is underestimated corresponding to the amount of $H_2^{35}S$, which was reoxidized to sulfate during incubation. Since the H_2S pool is non-labeled at the start of incubation and then builds up radioactivity according to an exponential saturation function, the reoxidation rate of $H_2^{35}S$ similarly builds up exponentially from zero to a saturation value. The initial $^{35}SO_4^{2-}$ reduction, measured as ^{35}S-accumulation in CRS + AVS (incl. H_2S), is therefore equal to the true *gross* rate of sulfate reduction ('Reduction' in Fig. 8A). As the H_2S pool gradually reaches the saturation level of radioactivity, the rate of $H_2^{35}S$ reoxidation grows and also reaches a saturation level. The rate of reduced ^{35}S accumulation falls to a correspondingly lower value, and a constant *net* rate of ^{35}S-sulfate reduction is observed (Fig. 8B). A sulfate reduction rate is then calculated, which reflects mostly the gross rate or the net rate, depending on the incubation time relative to the time constant for radiotracer saturation of the H_2S pool. Only a time course experiment can reveal this error, which shows up as an apparent decrease of the sulfate reduction rate with increasing incubation time or, correspondingly, as a cumulative formation of reduced ^{35}S which extrapolates back to a positive radioactivity at time zero (cf. Jørgensen 1978; Crill & Martens 1987). During long incubations, also the isotopic exchange and the binding of reduced ^{35}S in TRS may begin to level off.

The extent of underestimation of the true sulfate reduction due to concurrent $H_2^{35}S$ reoxidation has been calculated for the data in Fig. 1 (Table 1). In the oxidized 0–1.5 cm layer, the asymptotic net rate of sulfate reduction was 55 nmol SO_4^{2-} cm^{-3} d^{-1}, which was only about one fifth of the actual gross rate. The remaining four fifths of the ^{35}S reduced was rapidly reoxidized to sulfate from the dynamic H_2S pool. In the reduced and sulfidic sediment at 6–11 cm depth, however, the $H_2^{35}S$ reoxidation was insignificant and net and gross sulfate reduction were nearly similar. Although similar rates of

Table 1. Model calculations of Net and Gross Sulfate Reduction Rate (SRR) and H_2S reoxidation in two depth intervals of Aarhus Bay sediment, based on data from Fig. 1. For calculation formula: see Appendix.

Process	Calculation	0.0–1.5 cm	6–11 cm
		nmol S cm^{-3} d–1	
Net SRR	$p * [H_2S]$	55	42
H_2S reoxidation	$o * [H_2S]$	195	2
Gross SRR	$r * [SO_4^{-2}]$	250	44

(net) sulfate reduction were measured at 0–1.5 cm and 6–11 cm depth, the gross rate was by far the highest in the oxidized surface layer. These results are in accordance with earlier control experiments on the radiotracer method for sulfate reduction measurement, which have mostly been carried out with reducing, sulfidic sediments. In that case, a linear reduction rate may be found (Thode-Andersen & Jørgensen 1989), and also a good agreement between rates determined from radiotracer incubations or from direct measurements of sulfate depletion in the porewater (Crill & Martens 1987).

A rapid turnover of H_2S in the oxidized zone, either by reoxidation or by iron precipitation, can also be concluded independently from the high rates of sulfate reduction measured, 15–185 nmol SO_4^{2-} cm^{-3} d^{-1} (Fig. 6A). With such an average rate of H_2S formation, ca. 100 nmol cm^{-3} d^{-1}, and a H_2S pool of <1 μM, the turnover time must be <15 min.

The problem of choosing the incubation time for a correct radiotracer determination of sulfate reduction rate therefore mostly exists in the oxidized surface layer where the true rate may be seriously underestimated. The fact that much of the radiolabel from H_2S ends up in the vast TRS pool by isotopic exchange in fact helps to reduce this problem significantly by trapping the reduced ^{35}S. It thus improves the sulfate reduction determination, but at the same time it prevents the use of radiolabeled H_2S to study sulfide transformations (Fossing et al. 1992). The model presented here is a simplification of the sulfur cycling in the radio-tracer incubated sediment. Also components of the TRS pool, in particular freshly precipitated FeS or S°, may also be partly oxidized during incubation. The very simple model is maintained here, as experimental data to support modeling of a more complex sulfur cycle are lacking.

The processes included in the conceptual model of Fig. 8A have all been independently verified. Thus, the reoxidation of H_2S or FeS to sulfate in the anoxic zone of marine sediments, probably with Mn(IV) or Fe(III) com-

pounds as oxidants, has been demonstrated both chemically and by the use of ^{35}S-radiotracer (Aller & Rude 1988; Fossing & Jørgensen 1990a; dos Santos Afonso & Stumm 1992; Thamdrup et al. in press). A complete sulfide oxidation with Fe(III) may possibly take place via elemental sulfur, which may be disproportionated by bacteria to sulfate and sulfide rather than being directly oxidized to sulfate (Thamdrup et al. 1993; Canfield & Thamdrup, in press). The isotopic exchange between $H_2^{35}S$ and the particulate reduced sulfur species is partly catalyzed by polysulfides and is significant even within minutes of incubation (Fossing & Jørgensen 1990b). The decrease in apparent sulfate reduction rate with increasing incubation time was observed repeatedly during the six sampling occasions included in Fig. 1, but has, to different extents, also been noticed on many other occasions. An apparent linearity of sulfate reduction does not, however, exclude rapid H_2S reoxidation if the H_2S pool is very small and the transition time from gross to net rate therefore is too short to be noticed. Incubation times much shorter than 15 min are difficult to achieve due to the necessary time for experimental manipulations and for the radiotracer to diffuse and mix with the sulfate pools in the porewater and in the cells of sulfate reducing bacteria. Apparent non-linearity may also be due to $^{35}SO_4^{2-}$ contamination of the trapped $Zn^{35}S$ (Howarth & Jørgensen 1984) or to impurities in the radiotracer solution which are carried with the N_2 stream upon acidification and Chromium reduction (H. Fossing, personal communication). These artifacts are, however, revealed by inclusion of a zero-time sample.

As a consequence of the model calculations for the 0–1.5 cm surface zone, sulfate reduction in this suboxic layer may be 5-fold more important than anticipated. Of the total sulfate reduction in the 0–11 cm sediment layer, 35–55% of the activity (rather than 7–20% as calculated above) thus takes place in the top 1.5 cm. This conclusion agrees well with the observation of maximal densities of sulfate reducing bacteria in the oxidized surface layers of marine sediments in the adjacent Kattegat area (Jørgensen & Bak 1991). More detailed studies are required to clarify the rapid sulfur transformations in sediments and their effect on the results of radiotracer experiments.

Seasonal cycle. The seasonal variations in the mineralization rates and sediment chemistry are governed mainly by temperature, which varied between 4° (winter) and 15 °C (summer), and by sedimentation of algae from the overlying water column. The phytoplankton productivity varied from ca. 10 to 100 mmol C m^{-2} d^{-1} between winter and summer with a spring bloom productivity in May of up to 170 mmol C m^{-2} d^{-1} (County of Aarhus, unpublished data). Also, the partial oxygen depletion at the bottom of the stratified water column, with near-atmospheric saturation levels during winter and

spring but down to 25% saturation in late summer (Rasmussen & Jørgensen 1992), was important for the balance of aerobic and anaerobic mineralization processes. The pool sizes of pyrite and especially AVS showed a dynamic seasonal response in the top 0–1.5 cm but were rather constant throughout the year below that depth. The dynamics of the reduced sulfur and iron pools thus affected the seasonal variation in sulfide reoxidation and, thereby, in the fraction of the oxygen uptake involved in this reoxidation. During early summer, the pyrite pool increased rapidly and built up an 'oxygen debt' which enhanced the oxygen consumption during fall, when the pyrite was slowly oxidized again. The dynamic fraction of the pyrite pool at 0–1.5 cm was 150 mmol S m^{-2}, which could consume about 300 mmol of oxygen for its oxidation to sulfate. As the total oxygen uptake rate during summer was 15–20 mmol O_2 m^{-2} d^{-1} (Rasmussen & Jørgensen 1992), the reoxidation of pyrite could theoretically account for the total oxygen consumption over ca. two weeks. The build-up of an oxygen debt may thus play a role for the seasonal regulation of oxygen consumption, especially during periods of oxygen depletion in the water column. During periods of strong sediment resuspension, especially in late fall and winter, the oxidation of pyrite could cause a sudden enhanced oxygen uptake rate (H. Fossing, unpublished results).

The rapid development of a thin, black reducing zone at 2–4 mm depth, on top of the brown, oxidized surface sediment, was the consequence of a massive spring phytoplankton bloom sedimenting in April 1988 (Fig. 4A). This unique feature took place when the temperature was 5–7 °C and sulfate reduction rates were still generally low. It was not observed in the following year, when the spring bloom was less pronounced (Aarhus County Environmental Office, unpublished), but has been found on a nearby station in spring 1990 and later years (Thamdrup 1993; Thamdrup et al. in press). Measured sulfate reduction rates reached 64 nmol cm^{-3} d^{-1} in this zone, or more than twice the rates in the underlying, more oxidized sediment. If the rate measurements were affected by a concurrent reoxidation of sulfide, as shown by the model calculations above, the true rates in this surface layer may have been significantly higher (Table 1). The color change was due to a rapid iron reduction which led to a peak of free Fe^{2+} at 2–4 mm depth, just below the sulfate reduction maximum, and to a transient increase of ca. 10-fold in FeS concentration at 1–4 mm.

When integrated over the top 0–11 cm, sulfate reduction rates generally followed the seasonal temperature variations with a factor of 3.0 increase for 10 °C temperature increase over 5–15 °C (the 'seasonal Q_{10}'). This corresponds to an apparent activation energy of 73 kJ mol^{-1} in an Arrhenius equation and is within the range generally found for coastal sediments (Skyring 1987; Westrich & Berner 1988). In the 0–1.5 cm layer, the 'seasonal

Q_{10}' was 4–6, because of underestimation and inhibition of sulfate reduction in the oxidized layer during the cold winter months and less underestimation and enhanced sulfate reduction during the warm months. The term, 'seasonal Q_{10}', which includes seasonal variations in both environmental factors and microbial populations, is used here to distinguish is from the 'actual Q_{10}', which describes the temperature regulation of the microbial population at any given time. The 'actual Q_{10}' for sulfate reduction in the reducing sediment of Aarhus Bay was, however, also around 3 when measured at three different times of the year (B. B. Jørgensen, unpublished data).

The high rates of sulfate reduction combined with the relatively small seasonal variations in the reduced sulfur pools and with the lack of diffusible H_2S indicates that most of the sulfide oxidation takes place within the anoxic sediment, probably with nitrate, manganese, or iron as oxidants (cf. Aller & Rude 1988; King 1990; Fossing & Jørgensen 1990a; Elsgaard & Jørgensen 1992). It was recently estimated that bioturbation could quantitatively account for the vertical transport of Mn(IV), Fe(III), and sulfide minerals to make this anaerobic reoxidation a plausible mechanism (Thamdrup 1993; Thamdrup et al. in press). In spite of intensive sulfate reduction throughout the sediment layers studied, H_2S was detected (>1 μM) in the porewater only below 6–7 cm depth (Fig. 4B). The close coincidence between the extension of the H_2S zone and the lower boundary, where Fe^{2+} fell below 10 μM and where Fe^{HCl} levelled off at a low concentration, indicates a regulation of free H_2S by oxidation by Fe(III) and precipitation of iron sulfide minerals (cf. Pyzik & Sommer 1981; Giblin & Howarth 1984; Luther et al. 1992). The similarity between the isopleths of sulfate reduction and Fe^{2+} further indicates that much of the iron reduction was coupled to sulfide oxidation. Oxidation with Mn(IV) appeared to be restricted to 0–2 cm depth, where MnO_2 occurred at 10–100-fold lower concentrations than Fe(III), but probably with a much shorter turn-over time than the iron (Aller 1994; B. Thamdrup, unpublished). Another potential oxidant, nitrate, was found in the porewater down to only 3–8 mm, with the deepest penetration coinciding with the spring bloom (Lomstein et al. 1990).

The total sulfate reduction in the 0–11 cm sediment layer, calculated as the mean of the 40 min and 120 min incubations and integrated over the year, was 2.58 mol SO_4^{2-} m^{-2} y^{-1}. According to an average mineralization stoichiometry of two mol organic C per mol sulfate, (2 × 2.58 =) 5.16 mol m^{-2} y^{-1} of organic carbon could be oxidized through the measured sulfate reduction. The total annual oxygen uptake of the sediment over the same period, measured in laboratory-incubated cores, was 5.0 mol m^{-2} y^{-1} (erroneously calculated to be 10.1 mol m^{-2} y^{-1} in the paper of Rasmussen & Jørgensen (1992)). A similar seasonal study of the oxygen uptake rate

made two years later on a nearby, similar sediment station in the central Aarhus Bay resulted in an oxygen uptake rate of 6.6 mol m^{-2} y^{-1}. Both these estimates are, however expectedly underestimates of the *in situ* oxygen consumption because the uptake measurements did not include windy periods during which bottom currents, wave pumping, and sediment resuspension may significantly enhance oxygen uptake rates (Lund-Hansen et al. 1993; Valeur et al. in press; H. Fossing, unpublished results). Also the role of the benthic fauna for the total oxygen uptake tends to be underestimated in incubated sediment cores (Glud et al. in press). The total mineralization of organic matter can be estimated from the net deposition minus the burial of organic carbon in the area, as measured by sediment traps and ^{210}Pb-dating in 1990–91. This organic mineralization was 7.8 mol C m^{-2} y^{-1} (Valeur et al. 1992). Direct measurements of the CO_2-flux out of the sediment were also made over the seasons and yielded a rate of 9.8 mol C m^{-2} y^{-1} (B. A. Lomstein & T. H. Blackburn, unpublished), of which 1.2 mol may be due to carbonate dissolution (Valeur et al. 1992). Mineralization through sulfate reduction could thus account for about 2/3 of the oxidation of organic matter to CO_2.

The sedimentation rate in central Aarhus Bay is 0.09 g cm^{-2} y^{-1} corresponding to an accumulation rate of 1.7 mm y^{-1} at a depth of 11 cm (Lund-Hansen et al. 1993). The burial rate below 11 cm of accumulated pyrite, which is the main sulfur pool, is thus 0.21 mol m^{-2} y^{-1}, or 8% of the sulfide produced. The remaining 2.37 mol m^{-2} d^{-1} of the produced sulfide was consequently reoxidized. If oxygen were the terminal electron acceptor for the reoxidation of the 2.37 mol of sulfide, possibly with iron or manganese compounds as intermediate electron carriers, then ($2 \times 2.37 =$) 4.74 mol or most of the oxygen would be used for this purpose. As discussed above, the oxygen uptake measurements were probably underestimating the *in situ* rates.

In conclusion, the intensive seasonal study of sulfate reduction in Aarhus Bay sediments has confirmed its important role for the mineralization of organic matter and shown its close coupling to three factors: temperature, sedimentation, and iron geochemistry.

Acknowledgements

We thank Jens Støvlbæk for assistance with a mathematical model, Henrik Fossing for support in methodological questions, Don Canfield for a helpful discussion on the manuscript, and Preben Sørensen and Hans Jensen for help in the laboratory and at sea. The study was supported by the Danish Natural Science Council (to BBJ).

References

Aller RC (1994) The sedimentary Mn cycle in Long Island Sound: Its role as intermediate oxidant and the influence of bioturbation, O_2, and C_{org} flux on diagenetic reaction balances. J. Mar. Res. 52: 259–295

Aller RC & Rude PD (1988) Complete oxidation of solid phase sulfides by manganese and bacteria in anoxic marine sediments. Geochim. Cosmochim. Acta 52: 751–765

Aller RC, Mackin JE & Cox, Jr RT (1986) Diagenesis of Fe and S in Amazon inner shelf muds: apparent dominance of Fe reduction and implications for the genesis of ironstones. Continental Shelf Res. 6: 263–289

Bartlett JK & Skoog DA (1954) Colorimetric determination of elemental sulfur in hydrocarbons. Anal. Chem. 26: 1008–1011

Canfield DE (1988) Sulfate reduction and the diagenesis of iron in anoxic marine sediments. Ph.D. thesis, Yale University

Canfield DE & Des Marais DJ (1991) Aerobic sulfate reduction in microbial mats. Science 251: 1471–1473

Canfield DE & Thamdrup B. The production of ^{34}S depleted sulfide during the bacterial disproportionation of elemental sulfur. Science, in press

Canfield DE, Thamdrup B & Hansen JW (1993a) The anaerobic degradation of organic matter in Danish coastal sediments: Iron reduction, manganese reduction, and sulfate reduction. Geochim, Cosmochim. Acta 57: 3867–3883

Canfield DE, Raiswell R, Westrich JT, Reaves CM & Berner RA (1986) The use of chromium reduction in the analysis of reduced sulfur in sediments and shales. Chem. Geol. 54: 149–155

Canfield DE, Jørgensen BB, Fossing H, Guld R, Gundersen J, Ramsing NB, Thamdrup B, Hansen JW, Nielsen LP & Hall POJ (1993b) Pathways of organic carbon oxidation in three coastal sediments. Mar. Geol. 113: 27–40

Chao TT & Zhou L (1983) Extraction techniques for selective dissolution of amorphous iron oxides from soils and sediments. Soil Sci. Soc. Am. J. 47: 225–232

Cline JD (1969) Spectrophotometric determination of hydrogen sulfide in natural waters. Limnol. Oceanogr. 14: 454–458

Crill PM & Martens CS (1987) Biogeochemical cycling in an organic-rich coastal marine basin. 6. Temporal and spatial variations in sulfate reduction rates. Geochim. Cosmochim. Acta 51: 1175–1186

dos Santos Afonso M & Stumm W (1992) The reductive dissolution of iron(III)-(hydr)oxides by hydrogen sulfide. Langmuir 8: 1671–1676

Elsgaard L & Jørgensen BB (1992) Anoxic transformations of radiolabeled hydrogen sulfide in marine and freshwater sediments. Geochim. Cosmochim. Acta 56: 2425–2435

Fossing H & Jørgensen BB (1989) Measurement of bacterial sulfate reduction in sediments: Evaluation of a single-step chromium reduction method. Biogeochemistry 8: 205–222

Fossing H & Jørgensen BB (1990a) Oxidation and reduction of radiolabeled inorganic sulfur compounds in an estuarine sediment (Kysing Fjord, Denmark). Geochim. Cosmochim. Acta 54: 2731–2742

Fossing H & Jørgensen BB (1990b) Isotope exchange reactions with radiolabeled sulfur compounds in anoxic seawater. Biogeochemistry 9: 223–245

Fossing H, Thode-Andersen S & Jørgensen BB (1992) Sulfur isotope exchange between ^{35}S-labeled inorganic sulfur compounds in anoxic marine sediments. Mar. Chem. 38: 117–132

Fründ C & Cohen Y (1992) Diurnal cycles of sulfate reduction under oxic conditions in cyanobacterial mats. Appl. Environ. Microbiol. 58: 70–77

Giblin AE & Howarth RW (1984) Porewater evidence for a dynamic sedimentary iron cycle in salt marshes. Limnol. Oceanogr. 29: 47–63

Glud RN, Gundersen JK, Jørgensen BB, Revsbech NP & Schulz H. Diffusive and total oxygen uptake of deep-sea sediments in the south-east Atlantic Ocean: *In situ* and laboratory measurements. Deep-Sea Res., in press

Graf G, Bengtsson W, Diesner U & Theede H (1982) Benthic response to sedimentation of a spring phytoplankton bloom: process and budget. Mar. Biol. 67: 201–208

Hines ME, Bazylinski DA, Tugel JB & Lyons WB (1991) Anaerobic microbial biogeochemistry in sediments from two basins in the Gulf of maine: Evidence for iron and manganese reduction. Estuarine Coastal Shelf Sci. 32: 313–324

Howarth RW & Jørgensen BB (1984) Formation of ^{35}S-labeled elemental sulfur and pyrite in coastal marine sediments (Limfjorden and Kysing Fjord, Denmark) during short-term $^{35}S_4^{2-}$ reduction measurements. Geochim, Cosmochim. Acta 48: 1807–1818

Jensen MH, Andersen TK & Sørensen J (1988) Denitrification in coastal bay sediment: regional and seasonal variation in Aarhus Bight, Denmark. Mar. Ecol. Prog. Ser. 48: 155-162

Jørgensen BB (1978) A comparison of methods for the quantification of bacterial sulfate reduction in coastal marine sediments. I. Measurement with radiotracer techniques. Geomicrobiol. J. 1: 11–27

Jørgensen BB (1994) Sulfate reduction and thiosulfate transformations in a cyanobacterial mat during a diel oxygen cycle. FEMS Microbiol. Ecol. 13: 303–312.

Jørgensen BB & Bak F (1991) Pathways and microbiology of thiosulfate transformations and sulfate reduction in a marine sediment (Kattegat, Denmark), Appl. Environ. Microbiol. 57: 847–856

Jørgensen BB, Bang M & Blackburn TH (1990) Anaerobic mineralization in marine sediments from the Baltic Sea – North Sea transition. Mar. Ecol. Prog. Ser. 59: 39–54

King GM (1990) Effects of added manganic and ferric oxides on sulfate reduction and sulfide oxidation in intertidal sediments. FEMS Microbiol. Ecol. 73: 131–138

Kostka JE & Luther III GW (1994) Partitioning and speciation of solid phase iron in saltmarsh sediments. Geochim. Cosmochim. Acta 58: 1701–1710.

Lomstein E, Jensen MH & Sørensen J (1990) Intercellular NH_4^+ and NO_3^- pools associated with deposited phytoplankton in a marine sediment (Aarhus Bight, Denmark). Mar. Ecol. Prog. Ser. 61: 97–105

Lovley DR (1991) Dissimilatory Fe(III) and Mn(IV) reduction. Microbiol. Rev. 55: 259–287

Lovley Dr & Phillips EJP (1986) Organic matter mineralization with reduction of ferric iron in anaerobic sediments. Appl. Environ. Microbiol. 51: 683–689

Lovley DR & Phillips EJP (1987) Rapid assay for microbiology reducible ferric iron in aquatic sediments. Appl. Environ. Microbiol. 53: 1536–1540

Lund-Hansen LC, Pejrup M, Valeur J & Jensen A (1993) Gross sedimentation rates in the North Sea – Baltic Sea transition: effects of stratification, wind energy transfer, and resuspension. Oceanol. Acta 16: 205–215

Luther III GW, Kosta JE, Church TM, Sulzberger B & Stumm W (1992) Seasonal iron cycling in the salt-marsh sedimentary environment: the importance of ligand complexes with Fe(II) and Fe(III) in the dissolution of Fe(III) minerals and pyrite, respectively. Mar. Chem. 40: 81–103.

Pyzik AJ & Sommer SE (1981) Sedimentary iron monosulfides: kinetics and mechanism of formation. Geochim. Cosmochim. Acta 45: 687–698

Rasmussen H & Jørgensen BB (1992) Microelectrode studies of seasonal oxygen uptake in a coastal sediment: role of molecular diffusion. Mar. Ecol. Progr. Ser. 81: 289–303

Skyring GW (1987) Sulfate reduction in coastal ecosystems. Geomicrobiol. J. 5: 295–374

Sørensen J (1982) Reduction of ferric iron in anaerobic, marine sediment and interaction with reduction of nitrate and sulfate. Appl. Environ. Microbiol. 43: 319–324

Stookey LL (1970) Ferrozine – a new spectrophotometric reagent for iron. Anal. Chem. 42: 779–781

Thamdrup B (1993) Iron, Manganese, and Sulfur in the sea-floor – a biogeochemical study. Ph.D. thesis, University of Aarhus, Denmark

Thamdrup B, Finster K, Hansen JW & Bak F (1993) Bacterial disproportionation of elemental sulfur coupled to chemical reduction of iron or manganese. Appl. Environ. Microbiol. 59: 101–108

Thamdrup B, Fossing H & Jørgensen BB. Manganese, iron, and sulfur cycling in a coastal marine sediment (Aarhus Bay, Denmark). Geochim. Cosmochim. Acta, in press

Thode-Andersen S & Jørgensen BB (1989) Sulfate reduction and the formation of ^{35}S-labeled FeS, FeS_2, and S° in coastal marine sediments. Limnol. Oceanogr. 34: 793–806

Troelsen H & Jørgensen BB (1982) Seasonal dynamics of elemental sulfur in two coastal sediments. Estuar. Coast. Shelf Sci. 15: 225–266

Valeur JR, Jensen A & Pejrup M. Turbidity, particle fluxes and mineralization of C and N in a shallow coast area. Austr. J. Mar. Freshw. Res., in press

Valeur JR, Pejrup M & Jensen A (1992) Particulate nutrient fluxes in Vejle Fjord and Aarhus Bay (in Danish). Marine Research of the Environmental Agency, Vol. 14. The Danish Ministry of the Environment, Copenhagen. 127 pp

Westrich JT (1983) The consequences and controls of bacterial sulfate reduction in marine sediments. Ph.D. thesis, Yale University

Westrich JT & Berner RA (1988) The effect of temperature on rates of sulfate reduction in marine sediments. Geomicrobiol. J. 6: 99–117

Zhabina NN & Volkov II (1978) A method of determination of various sulfur compounds in sea sediments and rocks. In: Krumbein WE (Ed) Environmental Biogeochemistry and Geomicrobiology, Vol. 3 (pp 735–746). Ann Arbor Science Publishers, Michigan

Appendix

A theoretical model is presented here, with the purpose of explaining the non-linear time-course of ^{35}S accumulation in reduced sulfur pools during sulfate reduction measurements. The model builds on the following simplified assumptions (cf. Fig. 8):

- only the chemical pools of sulfate, free H_2S, and Total Reduced Sulfur (TRS = AVS + FeS_2 + S°) are considered; these chemical pools are designated [SO_4^{2-}], [H_2S], and [TRS]; they remain essentially constant over time, i.e. during a radiotracer experiment, the non-radioactive sulfur in the system is in steady state with respect to pool sizes and process rates,
- the corresponding pools of radioactive sulfur are designated $S^*O_4^{2-}$, H_2S^*, and TRS*,
- the radioactivity of the large sulfate pool remains constant during the experiment (in reality it decreases by <1 to a few percent),
- $S^*O_4^{2-}$ is reduced to H_2S^* with the rate constant, r,
- H_2S^* is oxidized to $S^*O_4^{2-}$ with the rate constant, o,
- H_2S^* is 'precipitated' as TRS* with the rate constant, p; this precipitation includes both the net transformation of H_2S^* into TRS* and the isotopic exchange of ^{35}S between H_2S^* and TRS* (cf. Fossing & Jørgensen 1990b; Fossing et al. 1992); the precipitation is considered irreversible during the initial accumulation of ^{35}S in TRS, i.e. throughout the incubation,
- 1'st order kinetics of radiotracer transformations are assumed throughout, i.e. rates are described by the rate constant times the pool size.

At time zero, all pools are non-radioactive. Labeled sulfate is then added in tracer amount and the pools of H_2S and TRS begin to accumulate radioactivity. The very small H_2S pool will most rapidly approach steady state radioactivity due to its fast turnover, whereas the large TRS pool slowly builds up radioactivity over a long period. The change of H_2S^* radioactivity over time, t, is then described by:

$$H_2S^*: \quad dH_2S^*/dt = rS^*O_4^{2-} - (o + p)H_2S^* \tag{1}$$

Equation (1) for H_2S^* is solved:

$$dH_2S^*/dt + (o + p)H_2S^* = rS^*O_4^{2-}$$

$$H_2S^* = rS^*O_4^{2-}/(o + p) + Ce^{-(o+p)t} \tag{2}$$

where C is an integration constant. Since the H_2S pool is non-radioactive at the start of the experiment, $H_2S^* = 0$ (and $e^{-(o+p)t} = 1$) for $t = 0$:

$$t_0: \quad H_2S^* = 0 = rS^*O_4^{-2}/(o+p) + C$$

$$C = -rS^*O_4^{-2}/(o+p)$$

which is inserted into (2):

$$H_2S^* = rS^*O_4^{-2}/(o+p) * (1 - e^{-(o+p)t}) \tag{3}$$

The change of TRS* radioactivity over time is described by:

$$\text{TRS}^*: \quad d\text{TRS}^*/dt = pH_2S^* \tag{4}$$

To solve this equation, the expression for H_2S^* from Equation (3) is inserted:

$$d\text{TRS}^*/dt = prS^*O_4^{2-}/(o+p) * (1 - e^{-(o+p)t})$$

$$\text{TRS}^* = prS^*O_4^{2-}/(o+p) * t + prS^*O_4^{2-}/(o+p)^2 * e^{-(o+p)t} + C' \tag{5}$$

Since also the TRS pool is non-radioactive at $t = 0$:

$$t_0: \quad \text{TRS}^* = 0 = prS^*O_4^{2-}/(o+p)^2 + C'$$

$$C' = -prS^*O_4^{2-}/(o+p)^2$$

This expression for C' is inserted into (5):

$$\text{TRS}^* = prS^*O_4^{2-}/(o+p) * t - prS^*O_4^{2-}/(o+p)^2 * (1 - e^{-(o+p)t}) \tag{6}$$

In the calculation of sulfate reduction rates from radiotracer experiments, the concentration of sulfate, $[SO_4^{-2}]$, is multiplied by the fraction of the radioactivity which has been reduced during incubation, $(H_2S^* + \text{TRS}^*)/S^*O_4^{-2}$. This fraction, F, can be calculated from Equations (3) and (6):

$$(H_2S^* + \text{TRS}^*) = prS^*O_4^{2-}/(o+p) * t + orS^*O_4^{2-}/(o+p)^2 * (1 - e^{-(o+p)t})$$

$$F = (H_2S^* + \text{TRS}^*)/S^*O_4^{-2} = pr/(o+p) * t + or/(o+p)^2 * (1 - e^{-(o+p)t}) \tag{7}$$

Equation (7) describes the time course of the relative radioactivity of reduced sulfur during incubation and has the form:

$$F = a + bt = ae^{-kt}$$

where,

$$a = or/(o+p)^2 \tag{8}$$

$$b = pr/(o+p) \tag{9}$$

$$k = o + p \tag{10}$$

Equations (8), (9), and (10) are solved for r, o and p:

$$r = ak + b \tag{11}$$

$$o = ak^2/(ak + b) \tag{12}$$

$$p = bk/(ak + b) \tag{13}$$

The curve for the function, F, goes through the origin, (0,0), and approaches the line, $a + bt$, asymptotically at increasing values of t. By curve-fitting to experimental data such as those in Fig. 1, the parameters, a, b, and k can be determined. From these parameters, the rate constants, r, o, and b, are then calculated according to Equations (11), (12), and (13).

Such a curve-fitting was made for the data in Fig. 1. The calculated rate constants, r, o, and p, were multiplied with pool sizes for SO_4^{2-} and H_2S in order to estimate the actual gross rates of sulfate reduction, the rates of sulfide reoxidation to sulfate, and, from the difference between the two, the net rates of sulfate reduction. It is only this net rate of sulfate reduction which is determined by the conventional calculation of sulfate reduction rates from ^{35}S experiments.

The porewater concentration of sulfate was nearly constant during the period with an average value of 23 mM. The concentration of free H_2S in the porewater was at or below the detection limit of 1 μM in the 0.0–1.5 cm interval. A maximum value of 1 μM was tentatively assumed in the calculation. For the depth interval of 6–11 cm, the mean H_2S concentration was 60 μM. The data presented in Table 1 were calculated based on these concentrations.

To check whether the rate constants calculated by curve-fitting to data in Fig. 1 were consistent with the pool sizes, the H_2S pool size at steady state was calculated from the well-defined sulfate pool using these rate constants:

$$[H_2S] = r/(o + p) * [SO_4^{2-}]$$

For the depth interval 0.0–1.5 cm, the derived $[H_2S]$ concentration was 0.8 μM, while for the depth interval 6–11 cm it was 54 μM. The good agreement with the measured value at 6–11 cm and the estimated value at 0.0–1.5 cm supports the internal consistency of the model and the estimated rate constants.

Based upon directly measured concentrations of the main sulfur compounds and upon known principles of transformations between compounds, the model may thus demonstrate or calculate:

1) why a non-linear time-course of ^{35}S-sulfate reduction is observed, when an extensive reoxidation of H_2S concurrently takes place,
2) the time constant of the initial transition period before a linear net reduction is approached,
3) the extent to which the radiotracer method by longer incubation times underestimates the gross rate of sulfate reduction,
4) the rate of H_2S reoxidation.

The extent to which all these points are fulfilled depends strongly upon the relative values of rate constants and pool sizes and on the quality of the experimental data.